The bandstop filter consists of two SRR layers, while the bandpass filter consists of two CSRR layers. Fabrication and testing techniques have been addressed to demonstrate these proof-of-concept devices. The first pass measurement data agree reasonably well with simulation predictions. Better agreement should be achieved with subsequent iterations and fabrication process characterization.

The measured bandstop filter achieves 30 dB in-band attenuation. Its principle mode of operation is by having the SRR providing a negative permeability and inhibiting wave propagation. The measured bandpass filter has an insertion loss of 2.5 dB, 3 dB bandwidth of 6%, and an attenuation slope of 20 dB/GHz. The bandpass characteristic comes from the CSRR providing both negative permeability and permittivity, and with the right tuning to impedance match to the dominant waveguide propagation mode. A more intuitive interpretation is to think of the two CSRR's and the waveguide walls in between as an inline leaky cavity resonator.

This work opens up new possibilities for very compact and light-weight waveguide filters. Other SRR or CSRR topologies with more splits or stubs can be used to tune the frequency and bandwidth. For example, a CSRR with four stubs is being investigated to form an orthogonal linear polarization to accommodate circular polarization applications. Alternatively, more layers with slightly different dimensions can be added to improve the bandwidth and attenuation slope.

ACKNOWLEDGMENTS

The authors thank Jimmy Takeuchi for the use of the waveguide filter test setup, Jean Nielsen and Mark Chisa for their help with samples fabrication. This work is funded by the United States Defense Advanced Research Projects Agency (DARPA) under contract #HR001-05-C-0068. United States Trademarks and Patent Office application is pending.

REFERENCES

1. D.R. Smith, W.J. Padilla, D.C. Vier, S.C. Nemat-Nasser, and S. Schultz, Composite medium with simultaneously negative permeability and permittivity, Phys Rev Lett 84 (2000), 4184–4187.
2. D. Schurig, J.J. Mock, B.J. Justice, S.A. Cummer, J.B. Pendry, A.F. Starr, and D.R. Smith, Metamaterial electromagnetic cloak at microwave frequencies, Science 314 (2006), 977–980.
3. T. Lam, C. Parazzoli, and M. Tanielian, Negative index metamaterial lens for the scanning angle enhancement of phased array antennas, In: S. Zouhdi, A. Sihvola, and A. Vinogradov (Eds.), Metamaterials and plasmonics: Fundamentals, modeling, applications, Springer, New York, NY, 2008, pp. 121–138.
4. P. Jin and R.W. Ziolkowski, Low-Q, electrically small, efficient near-field resonant parasitic antennas, IEEE Trans Antennas Propag 57 (2009), 2548–2563.
5. J.D. Baena, J. Bonache, F. Martin, R.M. Sillero, F. Falcone, T. Lopetegi, M. Laso, J. Garcia-Garcia, I. Gil, M.F. Portillo, and M. Sorolla, Equivalent-circuit models for split-ring resonators and complementary split-ring resonators coupled to planar transmission lines, IEEE Trans Microwave Theory Tech 53 (2005), 1451–1461.
6. R Marques, J.D. Baena, M. Beruete, F. Falcone, T. Lopetegi, M. Sorolla, F. Martin, and J. Garcia, Ab initio analysis of frequency selective surfaces based on conventional and complementary split ring resonators, J Opt A Pure Appl Opt 7 (2005), S38–S43.
7. J. Bonache, F. Martin, J. Garcia-Garcia, I. Gil, R. Marques, and M. Sorolla, Ultra wide bandpass filters (UWBPF) based on complementary split rings resonators, Microwave Opt Technol Lett 46 (2005), 283–286.
8. I.C. Hunter, L. Billonet, B. Jarry, and P. Guillon, Microwave filters-applications and technology, IEEE Trans Microwave Theory Tech 50 (2002), 794–805.
9. Available at: www.cst.com.
10. Available at: www.ansoft.com.

DIELECTRIC PROPERTIES CHARACTERIZATION OF HIGH DIELECTRIC CONSTANT THICK FILMS

Luciene S. Demenicis,[1] José Ignacio Marulanda,[2] Rodolfo A. A. Lima,[2] and Maria Cristina R. Carvalho[2]

[1] Instituto Militar de Engenharia - IME, Rio de Janeiro, Brazil

[2] Centro de Estudos em Telecomunicações, Pontifícia Universidade Católica do Rio de Janeiro - PUC-Rio, Rua Marquês de São Vicente, 225 - 22451-900 - Rio de Janeiro - RJ, Brazil; Corresponding author: mcris@cetuc.puc-rio.br

Received 21 December 2009

ABSTRACT: *A technique for the characterization of microwave dielectric properties of high dielectric constant thick films at room temperature is proposed, using multilayered coplanar waveguide transmission lines with high dielectric constant thick films deposited over the lines. Besides the simplicity, the technique allows the characterization of the films under similar conditions to those in which they will operate as compact devices in multilayered configurations. Time domain analysis and experimental results for 61-micron thick Barium Titanate films have confirmed the relative dielectric constant and loss tangent values (respectively, 100 and 0.3) predicted by the frequency domain characterization proposed.* © 2010 Wiley Periodicals, Inc. Microwave Opt Technol Lett 52:2339–2344, 2010; Published online in Wiley InterScience (www.interscience.wiley.com). DOI 10.1002/mop.25440

Key words: *microwave complex permittivity; dielectric characterization methods; thick films; coplanar waveguide; barium-titanate*

1. INTRODUCTION

High dielectric constant ceramics have emerged as key materials in the microwave industry due to an increasing need for higher power, smaller size, lighter weight, and lower cost frequency components [1]. Examples of applications in microwave engineering include tunable and miniaturized devices like varactors, resonators, phase shifters, filters, and antennas [2].

In the last few years, there has been active investigation for films with high dielectric constant and good performance at high frequencies, for use in microwave devices. The various possible applications range from compact devices in multilayer configurations [3, 4] to electrically tunable devices [5–9] in the case of ferroelectric ceramics. The design of microwave devices using multilayered film structures requires the accurate knowledge of the electrical characteristics of the film, such as dielectric constant and losses. It is well known that dielectric properties of such films are highly dependent of fabrication and characterization conditions, such as deposition methods and temperature, characterization frequency range, film thickness, etc [10]. It should be emphasized, then, that the characteristics of the film should ideally be obtained in the closest possible situation to the operation conditions. In practical applications, high dielectric constant materials are used as bulk ceramics, thick films or thin films and the dielectric properties have been measured depending on the form used [6].

Therefore, great effort has been directed to the appropriate characterization of such films. The choice of the measurement method and the correspondingly type of measurement setup strongly depends on the frequency range, on the form of the high dielectric constant material, and on the application of the final device. A comparison of film characterization techniques for microwave materials, involving coplanar waveguides (CPWs), coplanar resonators and interdigital capacitors (IDCs) made with high temperature superconductors printed over the film to be characterized was presented in [11], where good agreement among results for barium strontium titanate (BST) thin films was found. In [12], accurate measurement of BST-0.5 ($Ba_{0.5}Sr_{0.5}TiO_3$) thin-film based components and their characterization was performed using CPWs and IDCs, inferring the complex dielectric constant from scattering parameter measurements. In [13], a characterization method for measuring the complex permittivity of dielectric thin films is described, which uses a waveguide section partially filled with the substrate and the thin film. This method, however, does not take into account the multilayer effects.

Recently, a CPWs linear resonator technique has been proposed for the experimental characterization of the dielectric properties of films in the microwave frequency range at room temperature [14]. The technique was used to measure the dielectric constant and losses at microwave frequencies for various ceramic screen-printed thick films: $BaTiO_3$ (BTO), $CaCu_3Ti_4O_{12}$ (CCTO), and the composite BTO(x)-CCTO(1-x) with different concentration ratios ($x = 0.2$, 0.5, and 0.8).

It is noteworthy that in the herein presented configuration, and the above-mentioned CPW linear resonator configuration, the film lays over the CPW transmission line. There is a noticeable difference from the configurations seen in the previous mentioned characterization methods, where the line is printed over the film. When screen-printed thick films are considered, there is no metallization on the top face of the film. This is an advantage, as there is no great concern on the granularity of this surface, making film deposition simpler. Besides, the use of overlayered films line provides for better dispersion characteristics and lower impedance levels than the use of films underneath the line [15].

In this article, CPWs transmission lines with a dielectric film overlayer are used for the experimental characterization of the films. The film which dielectric constant is to be determined is deposited over a CPW transmission line printed on common alumina substrate. A direct measurement of the scalar scattering parameters of a set of lines with different lengths is performed. The effective parameters of the lines are evaluated from the characteristics of the insertion and return loss curves.

The effective dielectric constant results from the effects of both dielectrics and the line geometry. Comparison between experimental and theoretical results of the transmission and reflection characteristics of the lines in the frequency domain allows the determination of the film dielectric properties. The theoretical analysis of the lines was performed using a commercially available high-frequency structure simulator - ANSOFT HFSS - for the electromagnetic modeling of arbitrarily-shaped passive 3D structures [16]. A set of CPW lines was constructed and the characterization of BTO thick films was performed.

In addition, the effect of film losses on short electrical pulses propagating along the structures was carefully evaluated. A complete time domain analysis was performed with this multilayered device to confirm the measured propagation characteristics. Theoretical and experimental results of pulse distortion along the CPW with different lengths have been compared. Excellent agreement was obtained between the frequency characterization and the time-domain measurements.

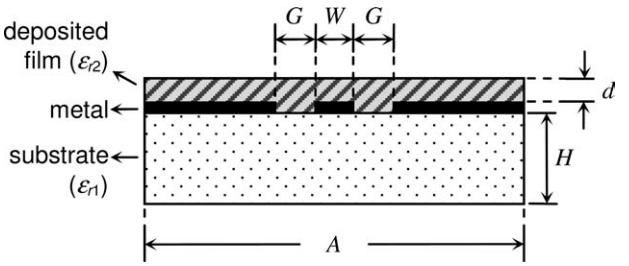

Figure 1 Schematic cross section of the CPW with overlayered film, showing the physical dimension parameters

2. FREQUENCY CHARACTERIZATION TECHNIQUE

Schematics and physical parameters of the overlayered CPW configuration used here are depicted in Figure 1. It consists of a CPW transmission line printed in gold metallization on a polished bulk alumina substrate (ε_{r1}) and covered with a thick film with very high relative dielectric constant (ε_{r2}). The cross section of the line can be observed in Figure 1, where the height H and width A of the substrate can be seen. The thickness d of the film is measured above the circuit metallization. Figure 1 also shows the CPW strip width W, and lateral gaps G. The line total length (not shown in the figure) will be denoted L.

The proposed technique is based on the measurement of the return and insertion losses of the CPW line under test, in the range between 0.05 and 20 GHz. From the return loss measurement it is possible to calculate the characteristic impedance of the line. At each integer multiple of half the wavelength, there is a perfect impedance matching, corresponding to the frequencies at which the return loss is minimum. Likewise, frequencies of maximum in this curve are related to the odd integer multiples of quarter-wavelengths. At these maximum points, of maximum mismatch, the input impedance equals the square of the line characteristic impedance divided by the load impedance (50 Ω in this case). The characteristic impedance of the line is then obtained from these values, which was also confirmed through time domain reflectometry measurements. Besides, it is well known that the insertion loss measurement for a CPW line yields the attenuation caused by the insertion of the transmission line, and consequently it is a means to calculate the loss tangent of the film [17].

For a given transmission line (i.e., geometry and substrate), the return and insertion loss curves are altered when a film is deposited over it. Measurements of the scattering parameters $|S_{11}|$ and $|S_{21}|$ at room temperature using a network analyzer are compared to a full wave spectral domain theoretical analysis performed in the application HFSS to obtain the film dielectric properties. When all physical dimensions of the line and film are known, comparison between measured results and theoretical predictions of reflection and transmission characteristics in the desired frequency range provides the dielectric constant and tangent loss of the film.

3. FREQUENCY DOMAIN EXPERIMENTAL RESULTS

The technique was employed in the measurement of the dielectric constant and losses at microwave frequencies for various ceramic screen-printed thick films of barium titanate ($BaTiO_3$–BTO). The CPW lines were fabricated on commercial thin-film polished alumina ($\varepsilon_{r1} = 9.8$ and $H = 635$ μm; Piconics), using conventional

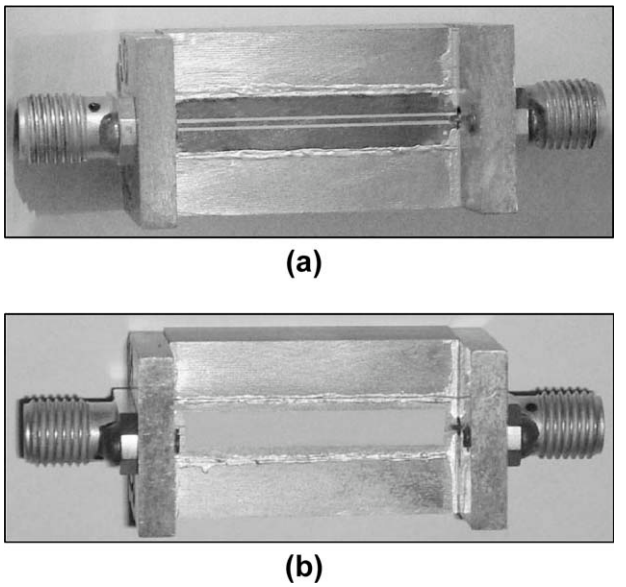

Figure 2 Prototype of the CPW lines constructed with length 25.4 mm: (a) without film; and (b) with overlayered thick film

photolithography process. The films under test were deposited over the respective lines by screen-printing technique, as described in [18]. The lateral CPW ground planes were fixed to the package with silver epoxy Epotek^{TM} H20E. Access to the circuit was performed using SMA connectors. An example of the 25.4-mm CPW prototypes without film constructed is shown in Figure 2(a), whereas Figure 2(b) displays a similar line with overlayered thick film.

Without loss of generality, all circuits constructed and measured in this work used the same transversal dimensions. According to Figure 1, the width of the alumina substrate used is $A = 5.0$ mm. The width of the CPW central line and lateral gap were dimensioned to yield 50-Ω line characteristic impedance in the absence of film, respectively $W = 500$ μm and $G = 210$ μm. Further, a set of lines with different values of total length L was constructed.

As a reference for the proposed method of frequency domain characterization, a baseline measurement without film was first performed on a 25.4-mm long 50-Ω CPW transmission line. A typical measured reflection characteristic (return loss) for the device is shown in Figure 3, obtained with an Agilent HP8720C vector network analyzer (0.05 to 20 GHz). According to the procedure described in Section 2, the −20 dB return loss observed in Figure 3 corresponds to a line characteristic impedance of ∼55 Ω. This value was confirmed by measurement with a time-domain reflectometer (TDR) model HP 1815B and sampler HP 1817A with 25-ps rise-time.

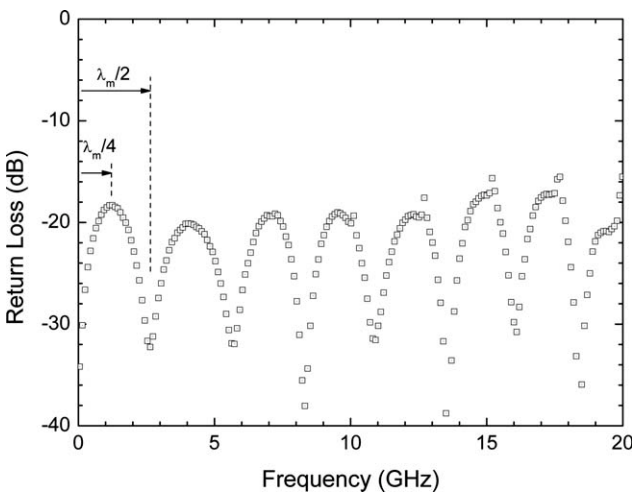

Figure 3 Measured return loss for a 25.4-mm long CPW transmission line without film

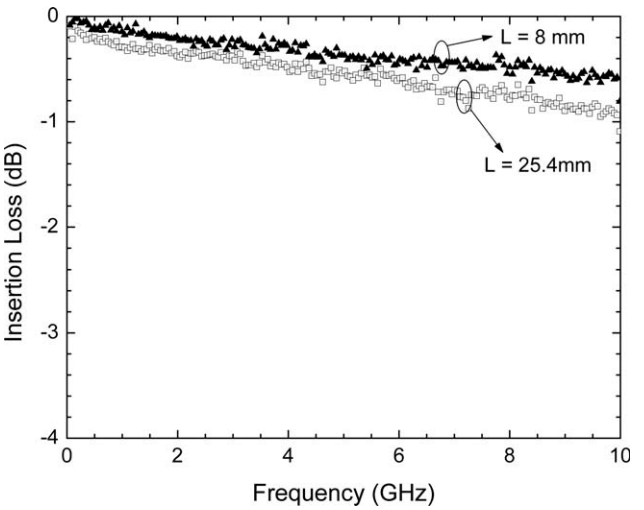

Figure 4 Measured insertion loss for two CPW transmission lines with lengths 8 and 25.4 mm, without film

To take into account the effects of mounting and fabrication imperfections, insertion loss for lines having different lengths must be measured [17]. Therefore, an 8-mm long CPW transmission line with identical transversal sections of the previous one is now considered. Figure 4 shows the insertion loss measured for both lines. The attenuation constant in dB per unit length was then calculated as the quotient of the difference between insertion loss values to the respective length difference, and is shown in Figure 5. It can be observed that the attenuation caused by the 55-Ω CPW line is less than 0.25 dB/cm up to 10 GHz in the absence of film.

The proposed technique was applied to the characterization of $BaTiO_3$ (BTO) films. The ceramic thick films were prepared

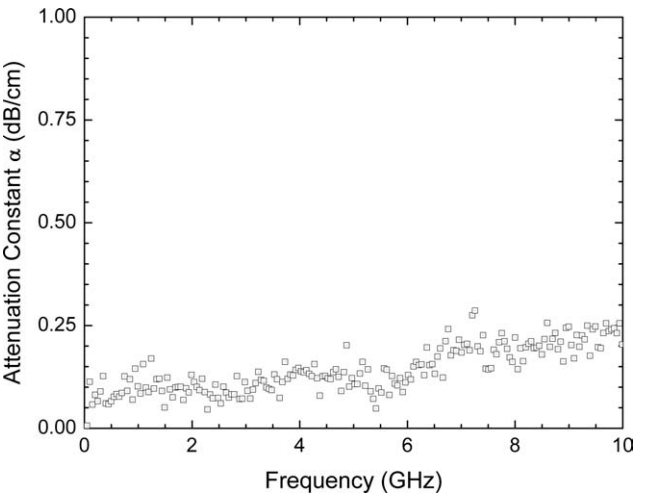

Figure 5 Experimental result for the attenuation constant (dB/cm) as a function of frequency for the fabricated CPWs, without film

according to the procedures described in [18]. To obtain the films under test, a paste was prepared from the suspension of organic material and the ceramic powder (BTO). A low-temperature melting material (flux material) was added in powder form to provide a better adherence between the paste and the bulk substrate and line. The measured thickness of the films was in the range of 50∼120 μm. They were characterized by X-ray diffraction, Raman Spectroscopy, Scanning Electron Microscopy (SEM), and Infrared Spectroscopy.

Considering that a 61-μm thick BTO film is deposited over the CPW line, major changes take effect on the return and insertion losses of the line. Figure 6 displays the curves of measured (solid line) and simulated (circles) return loss for the overlayered CPW line in this new configuration. Comparing the measurement of the plain 25.4-mm long CPW line, presented in Figure 3, with that of the film-overlayered line, in Figure 6, an excess attenuation can easily be observed in the latter one. This is particularly clear when examining the peaks of maximum return loss in Figure 6. Losses in the dielectric film introduce attenuation to the structure, which increases with frequency.

Moreover, the deposition of the film raised the effective dielectric constant and lowered the characteristic impedance of CPW line. These effects were expected, since the film has a very high permittivity. With the increase in effective dielectric constant, the frequency value corresponding to half wavelength downshifted from 2.5 to 1.4 GHz. From the value of the first maximum of the return loss curve (~ -5 dB) in Figure 6, it is verified that the level of the characteristic impedance of the line decreased to 25 Ω.

The theoretical results presented here were obtained from frequency domain simulation using the software application HFSS. In these simulations, a CPW line on alumina substrate with the same dimensions as the line in question was considered, and the characteristics of the dielectric film deposited over the line were adjusted as to optimally fit the measured results. The values obtained after this procedure were: relative permittivity $\varepsilon_{r2} = 100$ and loss tangent $\tan\delta_2 = 0.3$. The values used in the simulation described quite satisfactorily the behavior observed experimentally and agree with those obtained by measurements with the technique that uses linear CPW resonators presented in [14].

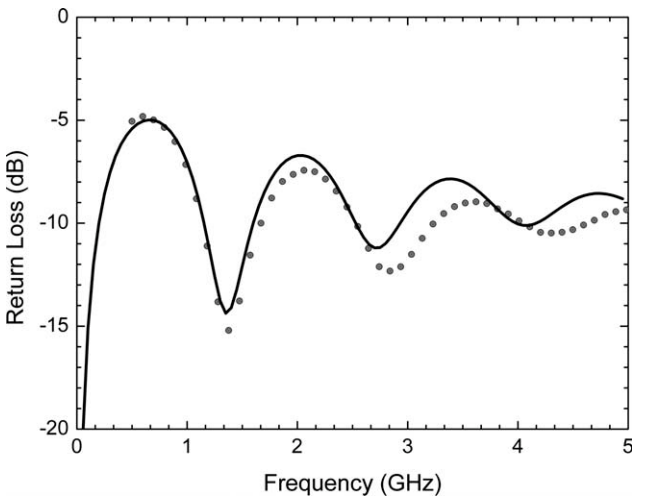

Figure 6 Return loss of a 25.4-mm long CPW transmission line with an overlayered 61-μm thick BTO film: comparison of measurement (solid line) and simulation (circles)

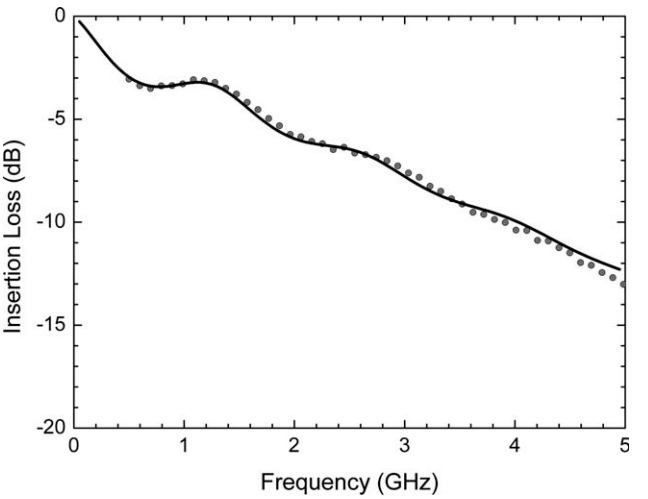

Figure 7 Insertion loss of a 25.4 mm long CPW transmission line with an overlayered 61-μm thick BTO film: comparison of measurement (solid line) and simulation (circles)

Regarding now the insertion loss of the same film-overlayered CPW line, Figure 7 presents the curves from both experimental measurement (solid line) and simulation (circles). Excellent agreement was found. A comparison of theoretical and measured results indicates again that the values used in the simulation describe accurately the behavior observed in practice.

Once again, two CPW transmission lines with identical cross section dimensions as the previous ones are considered, their lengths being 8 and 25.4 mm. This time, not only the effects of mounting and fabrication imperfections must be taken into account, but also the impedance mismatching between the 25-Ω line and the 50-Ω measurement equipment. Figure 8 shows the curves of the measured insertion loss for both lines. An insertion loss of 10 dB at 10 GHz is observed for the shorter line. Comparing the curves in Figure 8, a strong degradation of insertion loss is noticeable in the case of the longer line relatively to the shorter one. This large difference is due exclusively to the high dielectric losses of the film in the excess length of the longer line.

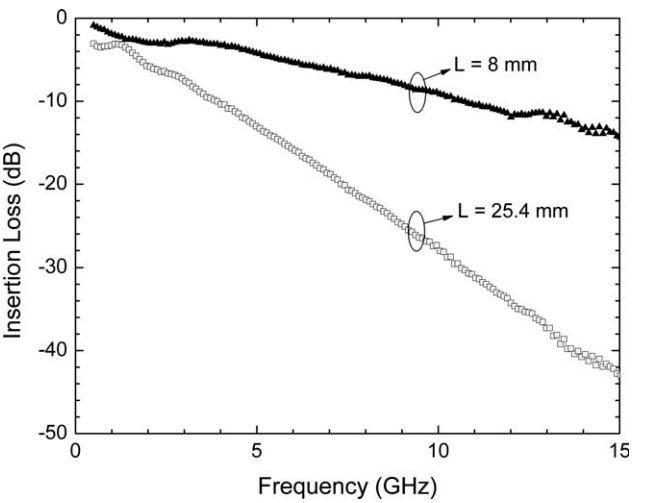

Figure 8 Measured insertion loss for two CPW transmission lines with an overlayered 61-μm thick BTO film, with lengths 8 and 25.4 mm

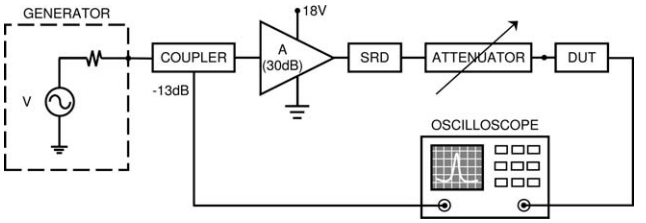

Figure 9 Block diagram of the experimental setup used for generating the short electrical pulses and measuring the device's time-domain response

4. TIME-DOMAIN ANALYSIS

In addition to the measurements of return and insertion losses, the time response of the prototype overlayered CPW lines in the configuration of Figure 1 was assessed, using short pulse excitation.

Short voltage pulses were generated using a recovery diode SRD (Step Recovery Diode). The schematic block diagram shown in Figure 9 illustrates the generation of a pulse train of 50 ps duration with a repetition rate of 1 GHz. The sinusoidal generator (HP83752B) operating at 1 GHz feeds the SRD (HP33005A). A small portion of the 0-dBm signal from the sine wave generator is used to trigger the digital oscilloscope (HP54120B; 50-GHz bandwidth), where the output signal is analyzed. The remaining signal goes through a 30-dB amplification to appropriately feed the SRD, yielding the pulse train. Figure 10 shows the voltage pulses obtained from this setup, with Gaussian shape, well balanced and with 50-ps duration at half height. The curve in Figure 10 was obtained in a direct configuration (without the DUT).

To obtain the time response of the film-overlayered CPW lines, the pulses were injected into one end of the overlayered CPW line and collected at the opposite end. The voltage pulses that traversed the line (the output pulses) were sampled at the oscilloscope. The results obtained for the 8-mm long line were then compared to the ones obtained for the 25.4-mm line. Figure 11 shows the output voltage pulses as a function of time, observed on the oscilloscope after going through each one of the CPW lines.

A time domain simulation of this multilayered device was performed to validate the previously measured propagation

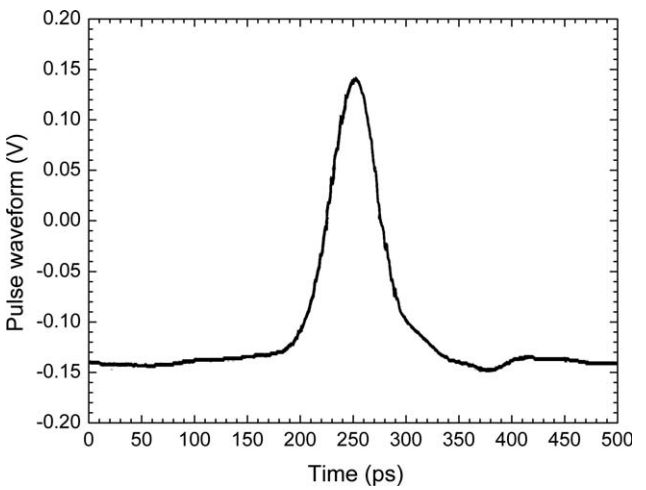

Figure 10 Generated input voltage pulses

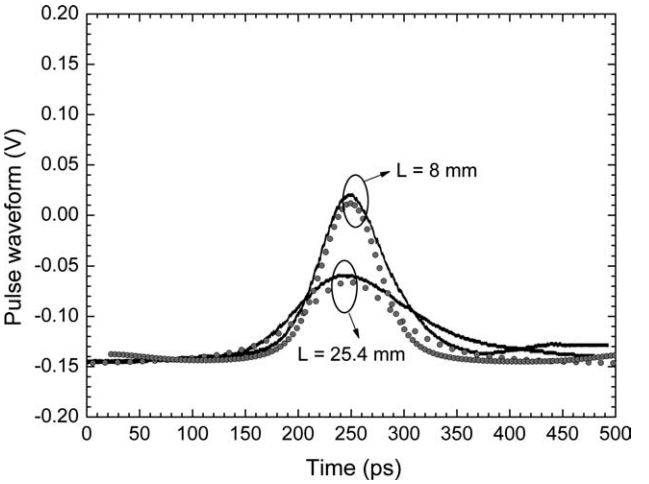

Figure 11 Voltage pulses in the output of the 8 and 25.4-mm long CPW transmission lines with an overlayered 61-μm thick BTO film: comparison of measurement (solid line) and simulation (circles)

characteristics. A mathematically generated gaussian pulse corresponding to the one in Figure 10 was injected in the modelled CPW transmission line [16, 19]. For comparison reasons, the results from the theoretical predictions were included in Figure 11. The amplitude attenuation of the voltage pulse due to film losses is more noticeable in the longer CPW line. In the 8-mm overlayered CPW line, the amplitude of the signal decreased one and a half times, whilst in the 25.4-mm line it dropped about three times with respect to the initial amplitude. The amplitude reduction yields the overall attenuation in the lines.

Comparing the results obtained experimentally with the simulations, it is possible to estimate the values of relative dielectric constant and losses of the BTO film from the assigned parameter values in the simulations. The values obtained for the dielectric constant (120 ± 25) and tangent loss (0.25 ± 0.05) are in good agreement with those found in Section 3, validating the techniques.

5. CONCLUSIONS

A technique for the characterization of microwave dielectric ceramic thick films was presented and tested. The technique is based on the confrontation of experimental measurements and simulated data, and provides simplicity and speed in getting the values of dielectric constant and loss tangent. In addition, it allows the characterization of the films under similar conditions to those in which they will operate. As discussed in this work, the similarity between the conditions for the characterization of films and conditions of use is crucial. Time domain measurements and analyses were also assessed for confirmation of the extracted film characteristics.

Using CPW transmission lines with deposited overlayered films, the dielectric constant and losses of BTO screen-printed thick films was investigated. A relative dielectric constant of 100 and a loss tangent of 0.3 at 10 GHz were obtained for 61-μm thickness BTO films. Excellent agreement between theoretical and experimental results was observed. The experimental results obtained by the time domain analysis have confirmed the frequency domain technique.

The proposed technique can be applied to transmission lines with different cross section configurations. It can also be extended to thin films with high values of relative dielectric

constant. Finally, a larger set of test fixtures will provide better accuracy in the characterization.

ACKNOWLEDGMENTS

This work was partially supported by Conselho Nacional de Desenvolvimento Científico e Tecnológico (CNPq) and by the Research and Development Center, Ericsson Telecomunicações S.A., Brazil.

REFERENCES

1. I.M. Reaney and D. Iddles, Microwave dielectric ceramics for resonators and filters in mobile phone networks, J Am Ceram Soc 89 (2006), 2063–2072.
2. S.J. Fiedziuszko, I.C. Hunter, T. Itoh, Y. Kobayashi, T. Nishikawa, S.N. Stitzer, and K. Wakino, Dielectric materials, devices and circuits, IEEE Trans Microwave Theory Tech 50 (2002), 706–720.
3. B.D. Lee, H.R. Lee, and K.H. Yoon, Effect of stacking layers on the microwave dielectric properties of $MgTiO_3/CaTiO_3$ multilayered thin films, J Am Ceram Soc 88 (2005), 1197–1200.
4. X.M. Chen, L. Li, and X. Q. Liu, Layered complex structures of $MgTiO_3$ and $CaTiO_3$ dielectric ceramics, Mater Sci Eng B 99 (2003), 255–258.
5. E. Marsan, J. Gauthier, M. Chaker, and Ke Wu, Tunable microwave device: Status and perspective, IEEE NEWCAS 3rd International Conference, Québec, 2005, pp. 279–282.
6. A.K. Tagantsev, V.O. Sherman, K.F. Astafiev, J. Venkatesh, and N. Setter, Ferroelectric materials for microwave tunable applications, J Electroceram 11 (2003), 5–66.
7. N. Setter, D. Damjanovic, L. Eng, G. Fox, S. Gevorgian, et al., Ferroelectric thin films: Review of materials, properties, and applications, J Appl Phys 100 (2006), 1–46.
8. A. Kozyrev, A. Ivanov, V. Keis, et al., Ferroelectric films: Nonlinear properties and applications in microwave devices, IEEE MTT-S Int Microwave Symp Digest 2 (1998), 985–988.
9. F.A. Miranda, F.W. Van Keuls, R.R. Romanofsky, C.H. Mueller, S. Alterovitz, and G. Subramanyam, Ferroelectric thin films-based technology for frequency and phase agile microwave communication applications, Integrated Ferroelectrics 42 (2002), 131–149.
10. S. Yun, X. Wang, and D. Xu, Influence of processing parameters on the structure and properties of barium strontium titanate ceramics. Mater Res Bull 43 (2008), 1989–1995.
11. P.M. Suherman, T.J. Jackson, and M.J. Lancaster, Comparison of techniques for microwave characterization of BST thin films, IEEE Trans Microwave Theory Tech 55 (2007), 397–401.
12. M. Ouaddari, S. Delprat, F. Vidal, M. Chaker, and Ke Wu, Microwave characterization of ferroelectric thin-film materials, IEEE Trans Microwave Theory Tech 53 (2005), 1390–1397.
13. B. Kim, V. Kazmirenko, Y. Prokopenko, Y. Poplavko, and S. Baik, Non-resonant, electrode-less method for measuring the microwave complex permittivity of ferroelectric thin films, Meas Sci Technol 16 (2005), 1792–1797.
14. L.S. Demenicis, R.A.A. Lima, L.F.M. Conrado, W. Margulis, and M.C.R. Carvalho, A CPW linear resonator method for the microwave characterization of high dielectric constant films, Microwave Opt Technol Lett 49 (2007), 521–524.
15. L.S. Demenicis, L.F.M. Conrado, W. Margulis, and M.C.R. Carvalho, Propagation characteristics of over-layered planar transmission line transformers, SBMO/IEEE MTT-S International Conference on Microwave and Optoelectronics, 2005, pp. 562–564.
16. HFSS™ 3D Full-wave electromagnetic field simulation, Ansoft Corp, Pittsburgh, PA.
17. K.C. Gupta, R. Garg, and I.J. Bahl, Microstrip lines and slotlines, Artech House, Washington, 1996.
18. A.F.L. Almeida, P.B.A. Fechine, J.C. Góes, M.A. Valente, M.A.R. Miranda, and A.S.B. Sombra, Dielectric properties of composite screen-printed thick films for high dielectric constant devices in the medium frequency (MF) range, Mater Sci Eng B 11 (2004), 113–123.
19. M.C.R. Carvalho and L.F.M. Conrado, Ultra-short-pulse propagation in arbitrarily terminated tapered planar lines for optoelectronics applications, Microwave Opt Technol Lett 22 (1999), 85–87.

BAND-PASS FILTERS USING HIGH-PERMITTIVITY CERAMICS SUBSTRATE

Cheng-Liang Huang,[1] Shin-Tung Tasi,[1] and Yuan-Bin Chen[2]

[1] Department of Electrical Engineering, National Cheng Kung University, 1 University Rd., Tainan 70101, Taiwan

[2] Department of Engineering and Management of Advanced Technology, Chang Jung Christian University, 396 Chang Jung Rd., Sec.1, Kway Jen, Tainan 71101, Taiwan; Corresponding author: cubnck@yahoo.com.tw

Received 21 December 2009

ABSTRACT: *The miniaturization of ring band-pass filters by employing high-permittivity ceramic substrates (with respective dielectric constants of 9.7 and 23.5) are investigated. Microwave dielectric ceramics with high-permittivity are commonly applied in several microwave communication components. With the advantages of compact size, high-permittivity ceramics can be used as the substrate for band-pass filters. Moreover, the fundamental characteristics of newly developed compact ring resonators have also been described and applied to the design of band-pass filters. In this article, the designed ring resonators structures are simulated using an HFSS simulator. The responses of the fabricated band-pass filters using* Al_2O_3 *(*$\varepsilon_r = 9.7$, $\tan\delta = 0.0001$*) and* $0.875Mg_{0.95}Zn_{0.05}TiO_3$-$0.125Ca_{0.8}Sm_{0.4/3}TiO_3$ *(*$\varepsilon_r = 23.5$, $\tan\delta = 0.000083$*) ceramic substrates are designed at the center frequency of 2.4 GHz. This compact size, low loss band-pass filter should be useful in many wireless communication systems.* © 2010 Wiley Periodicals, Inc.

Microwave Opt Technol Lett 52:2344–2347, 2010; Published online in Wiley InterScience (www.interscience.wiley.com). DOI 10.1002/mop.25439

Key words: *high-permittivity; band-pass filter; ceramics substrate*

1. INTRODUCTION

Microstrip ring resonators have many attractive features and can be used in satellites, mobile phones and other wireless communication systems. The main advantages of the resonators are their compact size, easy fabrication, narrow bandwidth, and low radiation loss. Therefore, the resonators are widely used in the design of filters, oscillators, and mixers. Due to the advantages of small size and easy fabrication, the microstrip ring resonators have been drawing much attention. Ceramic material with a high-quality factor ($Q \times f$) value (>10,000) and a high-permittivity provides a means to create small resonator structures, such as coaxial structures, which can be coupled to form combline band-pass filter [1]. However, Compact filters using microstrip ring resonators for cellular and other mobile communication systems have been reported [2].

The basic operation of the ring resonator based on the magnetic wall model was originally introduced by Wolff and Knoppik [3]. In addition, a simple mode chart of the ring was developed to describe the relation between the physical ring radius and resonant mode and frequency [4]. Although the mode chart of the magnetic wall model has been studied extensively, it provides only a limited description of the effects of the circuit parameters and dimensions [5]. A further study on a ring resonator using the transmission-line model was proposed [6]. The transmission-line model used a T-network in terms of equivalent